

# INDIRECT EPIPOLAR RESAMPLING OF SCENES USING PARALLEL PROJECTION MODELING OF LINEAR ARRAY SCANNERS

M. Morgan<sup>a</sup>, K. Kim<sup>b</sup>, S. Jeong<sup>b</sup>, A. Habib<sup>a</sup>

<sup>a</sup> Department of Geomatics Engineering, University of Calgary, Calgary, 2500 University Drive NW, Calgary, AB, T2N 1N4, Canada - (mfmorgan@ucalgary.ca, habib@geomatics.ucalgary.ca)

<sup>b</sup> Electronics and Telecommunications Research Institute (ETRI), 161 Gajeong-Dong, Yuseong-Gu, Daejeon, 305-350, Korea – (kokim, soo) @etri.re.kr

## PS WG III/1: Sensor Pose Estimation

**KEY WORDS:** Photogrammetry, Analysis, Modelling, Method, Pushbroom, Sensor, Stereoscopic, Value-added

### ABSTRACT:

Linear array scanners are used as a substitute of two-dimensional/frame digital cameras since they can produce high-resolution digital images comparable to scanned aerial photographs. On the other hand, digital frame cameras have inadequate size that is dictated by technical considerations/limitations. In general, rigorous sensor modelling involves the description of the physical process of data capture using such a sensor. For imaging systems, rigorous modelling incorporates the system's interior and exterior orientation parameters. Such parameters might not be always available for linear array scanners (e.g., commercially available IKONOS scenes). Deriving these parameters requires numerous ground control points. Moreover, the estimation process is geometrically ill posed due to the narrow angular field of view of the imaging system. Recently, parallel projection has emerged as an approximate model (for high altitude scanners with narrow angular field of view) that can be used to represent the mathematical relationship between scene and object space coordinates using few parameters. This paper outlines the derivation of resampling approach of linear array scanner scenes according to epipolar geometry. Conjugate points should have no  $y$ -parallax in the resampled scenes. Moreover, they should have an  $x$ -parallax that is linearly proportional to the corresponding object height. Such requirements can only be met by projecting the original scenes into a common horizontal plane. The paper explains the selection of such plane to meet these specifications. Experimental results using IKONOS data demonstrate the feasibility of the approach.

## 1. INTRODUCTION

Images generated according to epipolar geometry have the prime characteristic of having no  $y$ -parallax values. This fact makes them important prerequisite for many photogrammetric applications such as: automatic matching, automatic relative orientation, automatic aerial triangulation, automatic DEM generation, ortho-photo generation, and stereo viewing.

Two-dimensional digital cameras with large number of pixels comparable to scanned aerial photographs are not yet available. Therefore, linear array scanners are introduced to overcome this limitation by obtaining successive narrow coverage on the ground. Linear array scanners can be space-borne such as IKONOS, SPOT and MOMS, or airborne such as ASD-40. The high resolution and large coverage obtained by these scanners motivate their exploitation in performing photogrammetric activities, which could bring challenge to traditional topographic mapping with aerial images (Fritz, 1995).

In order to achieve highly accurate products, accurate geometric modelling has to be adopted. Two main categories of sensor modelling exist; rigorous and approximate modelling. The former describes the true geometry of the image formation and thus it is the most accurate model. Therefore, it has been frequently used in many applications (Lee and Habib, 2002; Habib et al., 2001; Lee et al., 2000; Wang, 1999; Habib and Beshah, 1998; McGlone and Mikhail, 1981; Ethridge, 1977). However, many ground control points are required for estimating the parameters associated with the rigorous model. In addition, the indirect determination of these parameters for space-borne scenes can be instable, due to the narrow angular

field of view (Wang, 1999). Furthermore, the parameters associated with the rigorous model can be concealed by the scene provide (e.g., IKONOS). As a result, other approximate models exist including the rational function model, the direct linear transformation, self-calibrating direct linear transformation and parallel projection (Tao and Hu, 2001; Ono et al., 1999; Wang, 1999; Abdel-Aziz and Karara, 1971).

Among these approximate models, the parallel projection model is adopted and utilized for epipolar resampling of linear array scanner scenes. Section 2 briefly discusses the epipolar resampling of frame cameras and introduces the linear array scanners. The reasons for choosing the parallel projection model and its mathematical formula are discussed in Section 3. Section 4 is dedicated for developing the epipolar resampling approach of linear array scanner scenes. Experimental results using IKONOS data are presented in Section 5. Finally, Section 6 includes the conclusions and recommendations for future work.

## 2. BACKGROUND

### 2.1 Epipolar Resampling of Frame Images

The main objective of epipolar resampling is to generate normalized images, which have the innate property that corresponding points lie on the same rows. Epipolar resampling of frame images is a straightforward process (Cho et al., 1992).

Figure 1 depicts two frame images at the time of exposure together with the normalized images. The resampling process necessitates projecting the original images onto a common

plane, whose orientation is determined by the orientation parameters of the original images. Moreover, original and normalized scenes share the same perspective centre. In this case, an object point,  $P$ , is projected onto the left and right normalized images as  $p$  and  $p'$ , respectively. Although the normalization process is straightforward when dealing with frame images, it is not possible using the rigorous modelling of linear array scanners as will be discussed in Section 2.3. But first, some terminologies for linear array scanners as well as their geometric modelling will be introduced.

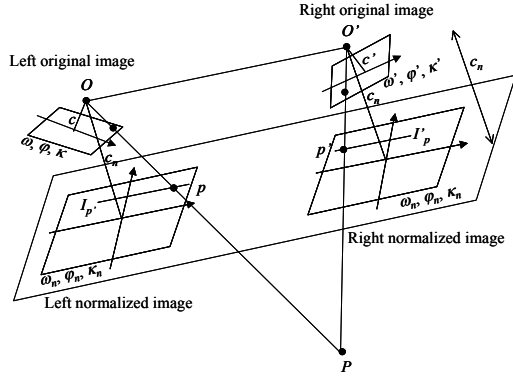


Figure 1. Epipolar resampling of frame images

## 2.2 Differences between Image and Scene

It is important to distinguish between the two terms “image” and “scene” throughout the analysis of linear array scanners, Figure 2.

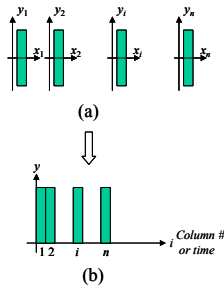


Figure 2. A sequence of 1-D images (a) constituting a scene (b)

An **image** is defined as the recorded sensory data associated with one exposure station. In the case of a frame image, it contains only one exposure station, and consequently it is one complete image. In the case of a linear array scanner, there are many 1-D images, each associated with a different exposure station. The mathematical model that relates a point in the object space and its corresponding point in the image space is the collinearity equations, which uses Exterior Orientation Parameters, EOP, of the appropriate image (in which the point appears).

In contrast, a **scene** is the recorded sensory data associated with one (as in frame images) or more exposure stations (as in linear array scanners) that covers near continuous object space in a short single trip of the sensor. Therefore, in frame images, the image and scene are identical terms, while in linear array scanners, the scene is an array of consecutive 1-D images.

## 2.3 Rigorous Modelling of Linear Array Scanners

Rigorous modelling of linear array scanners involves the scanner interior orientation parameters, IOP, and the exterior orientation parameters, EOP, for each image in the scene. Lee and Habib (2002) explicitly dealt with these parameters in pose estimation problems. Alternatively, other researchers reduced the number of involved parameters using functional representations of the EOP (Lee et al., 2000; Wang, 1999; McGlone and Mikhail, 1981; Ethridge, 1977). The underlying reason is that EOP do not abruptly change between consecutive images within the scene. For indirect estimation of the EOP using GCP, instability of the bundle adjustment exists, especially for space-based scenes (Wang, 1999; Fraser et al., 2001). This is attributed to the narrow Angular Field of View (AFOV) of space scenes, which motivates the investigation of the parallel projection model. Such a model will be discussed in more detail in the next section.

Before proceeding with the analysis of the parallel projection model, one has to note that rigorous modelling of linear array scanners does not allow straightforward epipolar resampling. One of the reasons is that it results in non-straight epipolar lines (Morgan et al., 2004a; Kim, 2000). However, in frame images, epipolar lines are straight in the original and normalized images (Cho et al., 1992). For this reason, a different model, parallel projection, will be sought for the analysis in Section 3.

## 3. PARALLEL PROJECTION

This section discusses the rationale behind selecting the parallel projection model. Linear and non-linear forms of the parallel projection model are presented. Finally, a prerequisite prior to handling scenes according to parallel projection is presented.

### 3.1 Motivations

The motivations for selecting the parallel projection model to approximate the rigorous model are summarized as follows, Figure 3:

- Many space scanners have narrow AFOV – e.g., it is less than  $1^\circ$  for IKONOS scenes. For narrow AFOV, the perspective light rays become closer to being parallel, Figure 3a.
- Space scenes are acquired within short time – e.g., it is about one second for IKONOS scenes. Therefore, scanners can be assumed to have the same attitude during scene capturing. As a result, the planes, containing the images and their perspective centres, are parallel to each other, Figure 3b.
- For scenes captured in very short time, scanners can be assumed to move with constant velocity. In this case, the scanner travels equal distances in equal time intervals. As a result, same object distances are mapped into equal scene distances, Figure 3c.

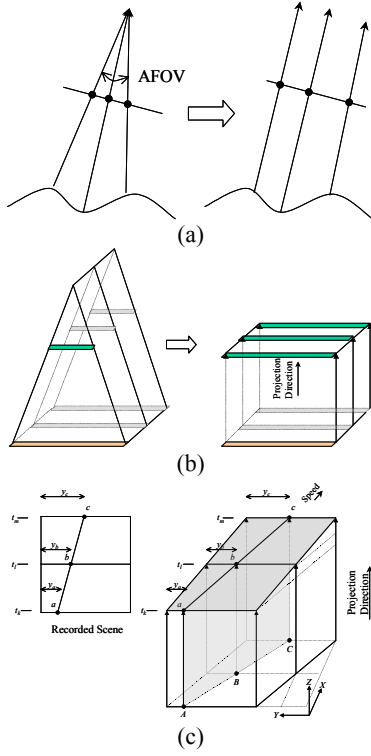


Figure 3. Motivations for using parallel projection

Therefore, many space scenes, such as IKONOS, can be assumed to comply with parallel projection. The next section presents the different forms of the parallel projection model.

### 3.2 Forms of the Parallel Projection Model

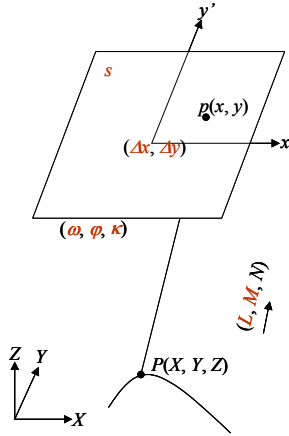


Figure 4. Parallel projection parameters

The parallel projection model, as shown in Figure 4, involves the following parameters:

- Two components of the unit projection vector ( $L, M$ );
- Orientation angles of the scene plane ( $\omega, \varphi, \kappa$ );
- Two shift values ( $\Delta x, \Delta y$ ); and
- Scale factor ( $s$ ).

The non-linear form of the parallel projection model relating an object point,  $P$ , to its scene point,  $p$ , can be expressed as:

$$\begin{bmatrix} x \\ y' \\ 0 \end{bmatrix} = s \cdot \lambda \cdot R^T \begin{bmatrix} L \\ M \\ N \end{bmatrix} + s \cdot R^T \begin{bmatrix} X \\ Y \\ Z \end{bmatrix} + \begin{bmatrix} \Delta x \\ \Delta y \\ 0 \end{bmatrix} \quad (1)$$

where:

$(X, Y, Z)$  are the object coordinates of the points of interest,  $P$ ;  
 $(x, y')$  are the scene coordinates of the corresponding point,  $p$ ;

$R$  is the rotation matrix between the object and scene coordinate systems;

$N$  is the Z-component of the unit projection vector - i.e.,  
 $N = \sqrt{1 - L^2 - M^2}$ ; and

$\lambda$  is the distance between the object and image points, which can be computed from the third equation in (1).

The linear form of the parallel projection model is derived by eliminating  $\lambda$  from Equations 1. It can be expressed as:

$$\begin{aligned} x &= A_1 X + A_2 Y + A_3 Z + A_4 \\ y' &= A_5 X + A_6 Y + A_7 Z + A_8 \end{aligned} \quad (2)$$

where  $A_1$  to  $A_8$  are the linear parallel projection parameters, and will be denoted as 2-D Affine parameters (Ono et al., 1999). It is important to mention that Equations 1 are useful if the scanner navigation data are available. On the other hand, if GCP are available, the linear model in Equations 2 becomes easier to use. The transformations between the linear and non-linear forms and their relation to the scanner navigation data are included in (Morgan et al., 2004b). One has to note that a parallel projection between two planes becomes 6-parameters standard Affine transformation. This can be easily seen if we consider planar object space (i.e., considering  $Z$  as a linear function of  $X$  and  $Y$  in Equations 2). The next subsection deals with a pre-requisite transformation prior to handling scenes according to parallel projection.

### 3.3 Perspective To Parallel (PTP) Transformation

Original scenes captured by linear array scanners conform to the rigorous perspective geometry along the scan lines. Therefore, before dealing with the parallel projection model, Perspective To Parallel (PTP) transformation of the scene coordinates are required. Such a transformation alters the scene coordinates along the scan lines to make them conform to the parallel projection (Ono et al., 1999), Equation 3.

$$y' = y \frac{1}{1 - \frac{y}{c} \tan(\psi)} \quad (3)$$

where:

$c$  is the scanner principal distance;

$\psi$  is the scanner roll angle; and

$y', y$  are the coordinates along the scan line according to parallel and perspective projection, respectively.

One has to note that Equation 3 assumes a flat terrain. In addition, it requires the knowledge of the scanner roll angle, which might (or might not) be available from the navigation data. Therefore, it is preferred to estimate the roll angle together with the parallel projection parameters using GCP. Combining the linear form of parallel projection and PTP transformation results in:

$$\begin{aligned} x &= A_1 X + A_2 Y + A_3 Z + A_4 \\ y &= \frac{A_5 X + A_6 Y + A_7 Z + A_8}{1 + \frac{\tan(\psi)}{c}(A_5 X + A_6 Y + A_7 Z + A_8)} \end{aligned} \quad (4)$$

The parameters in Equations 3 - i.e.,  $A_1$  to  $A_8$  and  $\psi$  - can be estimated using a minimum of five GCP. This model can be considered as a modified version of the parallel projection model, by taking into consideration the necessary PTP transformation. The next section deals with the utilization of the parallel projection parameters for epipolar resampling of linear array scanner scenes.

#### 4. EPIPOLAR RESAMPLING OF LINEAR ARRAY SCANNER SCENES

The epipolar line equation, adopting the parallel projection model, can be expressed as (Morgan, 2004; Ono et al., 1999):

$$G_1 x + G_2 y + G_3 x' + G_4 y' = 1 \quad (5)$$

where  $(x, y)$  and  $(x', y')$  are the coordinates of corresponding points in the left and right scenes, respectively. Four parameters,  $G_1$  to  $G_4$ , express the epipolar line equation. These parameters can be derived based on the 2-D Affine parameters or using point correspondences. In the latter case, at least four corresponding points have to be available.

From Equation 5, it can be easily seen that epipolar lines are straight in the parallel projection model. Furthermore, epipolar lines, in any of the scenes, are parallel to each other, Figure 5. Therefore, the epipolar line parameters can be utilized to transform the original scenes in such a way to eliminate the  $y$ -parallax values. One can consider rotating the scenes, each with different angle, to get the epipolar lines coinciding with the scene rows. Afterwards, scale and shift has to be applied to obtain corresponding epipolar lines along the same row. Such transformation can be expressed as:

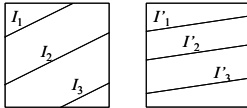


Figure 5. Epipolar lines in the parallel projection

$$\begin{aligned} \begin{bmatrix} x_n \\ y_n \end{bmatrix} &= \frac{1}{S} \begin{bmatrix} \cos(\theta) & \sin(\theta) \\ -\sin(\theta) & \cos(\theta) \end{bmatrix} \begin{bmatrix} x \\ y \end{bmatrix} + \begin{bmatrix} 0 \\ -\frac{\Delta y}{2} \end{bmatrix} \\ \begin{bmatrix} x'_n \\ y'_n \end{bmatrix} &= S \begin{bmatrix} \cos(\theta') & \sin(\theta') \\ -\sin(\theta') & \cos(\theta') \end{bmatrix} \begin{bmatrix} x' \\ y' \end{bmatrix} + \begin{bmatrix} 0 \\ \frac{\Delta y}{2} \end{bmatrix} \end{aligned} \quad (6)$$

where:

$(x_n, y_n)$  are the left scene coordinates after the transformation;

$(x'_n, y'_n)$  are the right scene coordinates after the transformation;

$\theta, \theta'$  are the rotation angles of the left and right scenes, respectively;

$-\Delta y/2, \Delta y/2$  are the shift values of the left and right scenes, respectively; and

$1/S, S$  are the scale factors of the left and right scenes, respectively.

It is important to note that Equation 5 contains only four parameters. Therefore, no more than four parameters can be introduced in Equations 6. Eliminating  $y$ -parallax (i.e., equating  $y'_n$  and  $y_n$ ) will result in an equation similar to Equation 5, but containing the four parameters  $\theta, \theta', \Delta y, S$ . By comparing these equations, one can derive the following equalities:

$$\begin{aligned} \theta &= \arctan\left(-\frac{G_1}{G_2}\right) \\ \theta' &= \arctan\left(-\frac{G_3}{G_4}\right) \\ S &= \sqrt{-\frac{G_3 \sin(\theta)}{G_1 \sin(\theta')}} = \sqrt{-\frac{G_4 \cos(\theta)}{G_2 \cos(\theta')}} \\ \Delta y &= -\frac{\sin(\theta)}{S.G_1} = \frac{\cos(\theta)}{S.G_2} = \frac{S.\sin(\theta')}{G_3} = -\frac{S.\cos(\theta')}{G_4} \end{aligned} \quad (7)$$

In summary, to eliminate  $y$ -parallax values, one has to derive the epipolar line parameters,  $G_1$  to  $G_4$ . Afterwards, the parameters  $(\theta, \theta', \Delta y, S)$  can be computed according to Equations 7. Finally, these parameters are used to rotate, scale and shift the scene coordinates according to Equations 6.

Although this procedure is successful in eliminating the  $y$ -parallax, it is not sufficient to produce useful stereopair. The problem is that the resulting  $x$ -parallax values are not in linear relationship with the height values (Morgan, 2004). By analyzing the transformations that were performed (rotation, shift and scale), it can be proven that they are planar. In other words, these transformations do not change the planes associated with the scenes. Recall that the scene planes are expressed by the rotation angles  $(\omega, \phi)$  in Equation 1.

To solve this problem, scenes have to be projected onto a common plane, similar to what have been discussed in frame images in Section 2.1. To select the orientation of this plane, *the normalization plane*, it is important to remember the main objective – that is to have linear relationship between  $x$ -parallax and height values. Figure 6 shows two points ( $B$  and  $D$ ) of same elevation and the parallel projection vectors  $(L, M, N)$  and  $(L', M', N')$  of the left and right scenes, respectively. It can be seen in this figure that only a horizontal plane (shown as dashed line) will maintain similar  $x$ -parallax values of points  $B$  and  $D$ . Therefore, scenes have to be projected onto a horizontal plane to maintain linear relationship between  $x$ -parallax and height.

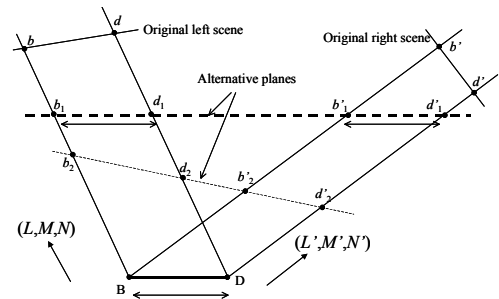


Figure 6. Selection of the normalization plane

Following this finding, the direction of epipolar lines within this plane can be determined. The parallel projection vectors, together with an object point, form a plane in space - *epipolar plane*. The direction of the epipolar lines can then be

determined by intersecting the epipolar plane with the normalization plane that is horizontal. Alternatively, it can be determined by intersecting it with the  $XY$ -plane, which results in a straight line along the vector  $(U, V, 0)$ , Figure 7. Therefore, the direction of the epipolar lines,  $\kappa_n$ , can be computed as:

$$\kappa_n = \arctan\left(\frac{V}{U}\right) = \arctan\left(\frac{N.M'-M.N'}{N.L'-L.N'}\right) \quad (8)$$

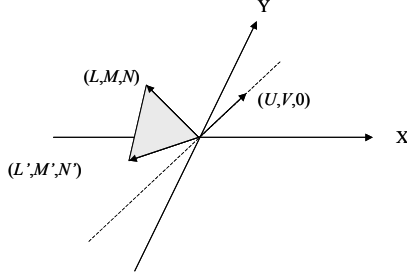


Figure 7. Direction of the epipolar lines

Utilizing the above findings, the indirect epipolar resampling approach of linear array scanner scenes can be summarized in the following steps (see Figure 8):

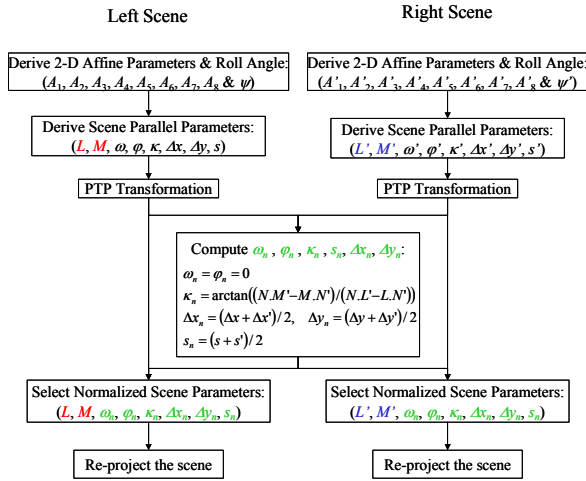


Figure 8. Epipolar resampling procedure

- For each scene, estimate the 2-D Affine parameters, together with scanner roll angles using GCP, adopting the model in Equations 4.
- For each scene, the roll angles are used for PTP transformation, and the parallel projection parameters are derived from the 2-D Affine parameters.
- The normalized scene parallel projection parameters are obtained by considering a horizontal plane (i.e.,  $\omega_n = \phi_n = 0$ ) and maintaining average scale and shift values, and rotating the scenes with an angle  $\kappa_n$  (Equation 8).
- The scenes are projected from their original parallel projection parameters to their normalized values. Such a transformation is considered as parallel projection between two planes (which is considered a 6-parameter Affine transformation as discussed in Section 3.2).

## 5. EXPERIMENTS

A panchromatic stereopair of IKONOS scenes covering Daejeon, South Korea is used in the experiments. The geographical coordinates of the area range from 36.26° to 36.36° North Latitude and from 127.31° to 127.45° East Longitude. An overview of these scenes is shown in Figure 9. The number of rows and columns and the acquisition data/time of the scenes are listed in Table 1.

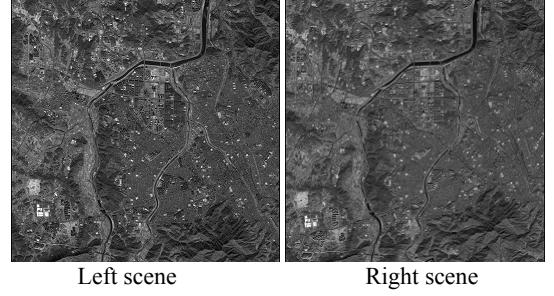


Figure 9. Overview of the IKONOS scenes

|                   | Left       | Right      |
|-------------------|------------|------------|
| Number of rows    | 13824      | 14336      |
| Number of columns | 13816      | 13816      |
| Acquisition date  | 2001-11-19 | 2001-11-19 |
| Acquisition time  | 02:18 GMT  | 02:19 GMT  |

Table 1. IKONOS scenes' dimensions and acquisition data/time

No information regarding the roll angles of the scenes and no GCP were available. Instead, the rational function coefficients of each of the scenes were provided. They were used to derive the ground coordinates of measured tie points - 162 points in total (Tao and Hu, 2002). A coordinate transformation was then implemented to obtain GCP in the local Cartesian coordinate system. Three sets of experiments were tested using different numbers of GCP and check points, Table 2. The developed approach for epipolar resampling was then performed. The square root of the estimated variance components, adopting Equations 4, and the average absolute values of the resulting  $y$ -parallax are listed in Table 2. The means and standard deviations of the error values in the object space are also listed in the same table.

| Experiment                      |                                     | 1                 | 2                 | 3                 |
|---------------------------------|-------------------------------------|-------------------|-------------------|-------------------|
| # of GCP                        |                                     | 9                 | 25                | 162               |
| # of Check points               |                                     | 153               | 137               | 0                 |
| $\hat{\sigma}_0$ _Left, pixels  |                                     | 4.8               | 3.7               | 2.9               |
| $\hat{\sigma}_0$ _Right, pixels |                                     | 1.7               | 1.3               | 1.1               |
| Mean/ $P_v$ , pixels            |                                     | 2.3               | 1.6               | 1.5               |
| GCP                             | Mean $_{xy} \pm \text{Std}_{xy, m}$ | 0.000 $\pm$ 1.707 | 0.000 $\pm$ 0.993 | 0.000 $\pm$ 0.889 |
|                                 | Mean $_z \pm \text{Std}_z, m$       | 0.000 $\pm$ 5.674 | 0.000 $\pm$ 6.086 | 0.000 $\pm$ 5.450 |
| Check points                    | Mean $_{xy} \pm \text{Std}_{xy, m}$ | 0.103 $\pm$ 1.364 | 0.095 $\pm$ 0.930 | -                 |
|                                 | Mean $_z \pm \text{Std}_z, m$       | 1.588 $\pm$ 6.101 | 0.587 $\pm$ 5.491 | -                 |

Table 2. Experimental results of the normalization process

From Table 2, an insignificant improvement between Experiments 2 and 3 can be seen. Thus, it can be concluded that few GCP can be used for epipolar resampling according to the approach developed in this research. In addition, error standard deviation values of the check points are not significantly different from those of the GCP. Therefore, the suggested approaches achieve similar errors throughout the resulting



normalized stereopair. In other words, errors 'far from' the GCP are similar to those 'close to' the GCP. The resampled scenes are overlaid to generate a stereo anaglyph (see Figure 10), which can be stereo-viewed using anaglyph glasses.

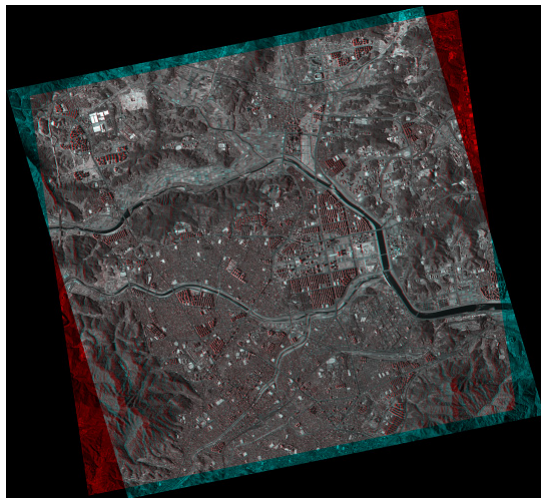


Figure 10. Stereo anaglyph of the normalized scenes

## 6. CONCLUSIONS AND RECOMMENDATIONS

In this paper, parallel projection is chosen to model space-borne scenes such as IKONOS. The rationale behind selecting this model is that many space scenes have narrow AFOV and acquired in very short time. Because the original scenes conform to the rigorous perspective geometry, scene coordinates along the scan lines have to be altered in PTP transformation so that they conform to the parallel projection. The parallel projection model is discussed together with its linear and non-linear forms. The former is preferred when GCP are available while the latter is preferred when navigation data are available. A modified parallel projection model that combines the linear form and PTP transformation is presented. The advantage of this model is that it can be used to indirectly estimate the required scene parameters using only GCP. Finally, the epipolar resampling procedure of linear array scanner scenes is briefly presented, which eliminates  $y$ -parallax values and maintains linear relationship between  $x$ -parallax and height values. Experimental results using IKONOS data showed the feasibility and success of the epipolar resampling procedure.

Future work will include testing different data such as SPOT scenes. In addition, direct versus indirect procedures for epipolar resampling will be compared in terms of the achieved accuracy. Inclusion of higher order primitives (such as linear and areal features) and object space constraints to the parallel projection model will be analyzed. Finally, DEM and orthophotos will be generated based on the normalized scenes.

## REFERENCES

Abdel-Aziz, Y., and H. Karara, 1971. Direct Linear Transformation from Comparator Coordinates into Object Space Coordinates in Close-Range Photogrammetry, *Proceedings of ASP/UI Symposium on CloseRange Photogrammetry*, University of Illinois at Urbana Champaign, Urbana, Illinois, pp. 1-18.

Cho, W., T. Schenk, and M. Madani, 1992. Resampling Digital Imagery to Epipolar Geometry, *IAPRS International Archives of Photogrammetry and Remote Sensing*, 29(B3): 404-408.

Ethridge, M., 1977. *Geometric Analysis of Single and Multiply Scanned Aircraft Digital Data Array*, PhD Thesis, Purdue University, West Lafayette, Indiana, 301p.

Fraser, C., H. Hanley, and T. Yamakawa, 2001. Sub-Metre Geopositioning with IKONOS GEO Imagery, *ISPRS Joint Workshop on High Resolution Mapping from Space*, Hanover, Germany, 2001.

Fritz, L., 1995. Recent Developments for Optical Earth Observation in the United States, *Photogrammetric Week*, pp75-84, Stuttgart, 1995.

Habib, A. and B. Beshah, 1998. Multi Sensor Aerial Triangulation, *ISPRS Commission III Symposium*, Columbus, Ohio, 6 – 10 July, 1998.

Habib, A., Y. Lee, and M. Morgan, 2001. Bundle Adjustment with Self-Calibration of Line Cameras using Straight Lines. *Joint Workshop of ISPRS WG I/2, I/5 and IV/7: High Resolution Mapping from Space 2001*, University of Hanover, 19-21 September, 2001.

Kim, T., 2000. A Study on the Epipolarity of Linear Pushbroom Images, *Journal of Photogrammetric Engineering & Remote Sensing*, 66(8): 961-966.

Lee, Y., and A. Habib, 2002. Pose Estimation of Line Cameras Using Linear Features, *ISPRS Symposium of PCV'02 Photogrammetric Computer Vision*, Graz, Austria.

Lee, C., H. Theiss, J. Bethel, and E. Mikhail, 2000. Rigorous Mathematical Modeling of Airborne Pushbroom Imaging Systems, *Journal of Photogrammetric Engineering & Remote Sensing*, 66(4): 385-392.

McGlone, C., and E. Mikhail, 1981. Photogrammetric Analysis of Aircraft Multispectral Scanner Data, *School of Civil Engineering, Purdue University*, West Lafayette, Indiana, 178p.

Morgan, M., 2004. *Epipolar Resampling of Linear Array Scanner Scenes*, PhD Dissertation, Department of Geomatics Engineering, University of Calgary, Canada.

Morgan, M., K. Kim, S. Jeong, and A. Habib, 2004a. Epipolar Geometry of Linear Array Scanners Moving with Constant Velocity and Constant Attitude, *XX<sup>th</sup> Congress of ISPRS*, 12-23 July, 2004.

Morgan, M., K. Kim, S. Jeong, and A. Habib, 2004b. Parallel Projection modelling for Linear Array Scanner scenes, *XX<sup>th</sup> Congress of ISPRS*, 12-23 July, 2004.

Ono, T., Y. Honmachi, and S. Ku, 1999. Epipolar Resampling of High Resolution Satellite Imagery, *Joint Workshop of ISPRS WG I/1, I/3 and IV/4 Sensors and Mapping from Space*.

Tao, V. and Y. Hu, 2001. A Comprehensive Study for Rational Function Model for Photogrammetric Processing, *Journal of Photogrammetric Engineering & Remote Sensing*, 67(12):1347-1357.

Wang, Y., 1999. Automated Triangulation of Linear Scanner Imagery, *Joint Workshop of ISPRS WG I/1, I/3 and IV/4 on Sensors and Mapping from Space*, Hanover, 1999.